Materials Science-Poland, *Vol. 27*, *No. 2*, *2009*

Influence of antimony oxide on the dielectric properties of barium strontium titanate based ceramics

C. ZHANG*, Y. QU

Key Laboratory for Advanced Ceramics and Machining Technology of Ministry of Education, Tianjin University, Tianjin 300072, P. R. China

The dielectric properties of Sb_2O_3 doped $(Ba_{0.992-x}Sr_xDy_{0.008})TiO_{3.004}$ ceramics fabricated by a solid state route with various Sb_2O_3 contents and Sr/Ba ratios were investigated. The XRD patterns confirm the samples to be multiphase compounds composed of perovskite major phase and $Ba_4Ti_{13}O_{30}$, $Ba_6Ti_{17}O_{40}$, Ti_7O_{13} secondary phases. The average lattice constant indicates that Sb^{3+} ions initially occupy the A-sites and then enter the B-sites serving as acceptor dopants. The Curie temperature decreases as the Sb_2O_3 content increases and as the Sr/Ba ratio increases also. The thermal stability of the electric permittivity increases as the Sb_2O_3 concentration increases but decreases as the Sr/Ba ratio increases. The resistivity and ac standing voltage decrease as the Sr/Ba ratio decreases. The Sb_2O_3 doped $(Ba_{0.992-x}Sr_xDy_{0.008})TiO_{3.004}$ ceramics with high permittivity, low dielectric loss, high ac standing voltage and low temperature coefficient of capacitor are obtained for applications in environment friendly capacitors.

Key words: *barium strontium titanate; doping effects; dielectrics; capacitors*

1. Introduction

Barium titanate ceramics has been used extensively as capacitor dielectrics for the past few decades [1]. Barium strontium titanate ($Ba_{1-x}Sr_xTiO_3$, hereafter referred to as BST) as a solid solution composed of barium titanate and strontium titanate has received intensive attention due to its high electric permittivity, low dissipation factor and adjustable Curie temperature [2–6]. Doping effects of various oxides on barium strontium titanate ceramics have also been reported [7, 8]. Incorporating rare earth oxides into the perovskite structure is an effective way to improve dielectric properties of barium strontium titanate ceramics. According to Huang [9], Dy_2O_3-doped BST capacitor ceramics possess a high permittivity (ε = 5245), low dielectric loss (tanδ

*Corresponding author, e-mail: zhch1234581@hotmail.com

= 0.0026) and high dc breakdown voltage (E_b = 5.5 MV/m). Zhao et al. [10] also reported that significantly new properties (ε = 3658, tanδ = 0.0093, $\Delta\varepsilon/\varepsilon$ = 14.1%) were obtained in Y_2O_3 and Dy_2O_3 doped BST ceramics.

Many rare earth elements are confirmed to act as donors in $BaTiO_3$ perovskite structure within a certain doping concentration. According to Kim [11], Y_2O_3 initially entered the A sites (< 1.0 mol %) in Ba excess $BaTiO_3$ ceramics and then occupied the B sites (>1.0 mol %) as acceptors. With the increase in the Sm_2O_3 doping content in $BaTiO_3$ ceramics, the following two defect reactions occurred successively and then another phase belonging to $P6_322$ space group appeared [12]:

$$2Sm_2O_3 + 4TiO_2 \rightarrow 4Sm^{\bullet}_{Ba} + 4Ti_{Ti} + 12O_O + O_2 + 4e' \quad (1)$$

$$2Sm_2O_3 + 6TiO_2 \rightarrow 4Sm^{\bullet}_{Ba} + 6Ti_{Ti} + 18O_O + 2V''_{Ba} \quad (2)$$

The substitution characteristics of Dy_2O_3 in barium titanate ceramics are similar to those of Y_2O_3. The substituting mechanism can be expressed as follows [13]:

$$xDy^{3+} + BaTiO_3 \rightarrow (Ba^{2+}_{1-x}Dy^{3+}_x)[Ti^{4+}_{1-x}(Ti^{4+}\cdot e)_x]O_3 + xBa^{2+} \quad (3)$$

$$xDy^{3+} + BaTiO_3 \rightarrow Ba^{2+}_{1-x/2}Dy^{3+}_x(Ti^{4+}_{1-x/2})O_3 + (x/2)Ba^{2+} + (x/2)Ti^{4+} \quad (4)$$

Antimony oxide is one of the common additives in $BaTiO_3$ based ceramics with positive temperature coefficient of resistance (PTCR). The effects of Sb_2O_3 addition on the PTCR properties of BST ceramics have been investigated [14]. Unfortunately, there have been few reports concerning the effects of antimony oxide on the dielectric properties of BST ceramics. In the previous work, we have studied the dielectric properties of Sb_2O_3 doped $(Ba_{0.992-x}Sr_xY_{0.008})TiO_{3.004}$ ceramics [15]. In this study, we continue to prepare the Sb_2O_3 doped $(Ba_{0.992-x}Sr_xDy_{0.008})TiO_{3.004}$ dielectrics by solid state reaction technique. The purpose of this paper is to investigate the influence of antimony oxide on the structural and the dielectric properties of $(Ba_{0.992-x}Sr_xDy_{0.008})TiO_{3.004}$ ceramics, as well as to provide a class of fine capacitor ceramics possessing high electric permittivity, low dielectric loss, high breakdown voltage and low temperature coefficient of the capacitor.

2. Experimental

The chemical compositions of the specimens are shown in Table 1. High purity $BaCO_3$ (>99.0%), $SrCO_3$ (>99.0%), TiO_2 (>98.0%) and Dy_2O_3 (>99.0%) powders, used as raw starting materials, were weighed, ball-milled, dried and calcined at 1080 °C for 2 h. The calcined powders were mixed with Sb_2O_3 (>99.0%), reground, dried and

added with 5 wt. % polyvinyl alcohol (PVA) as a binder for granulation. The granulated powders were sieved through a 40 mesh screen and then pressed into pellets (Φ12 mm×2 mm) under 250 MPa. Sintering was conducted in air at 1300 °C for 2 h. For dielectric measurement, both flat surfaces of the specimens were coated with silver paste. Finally, the painted samples were fired at 610 °C for 10 min.

Table 1. Chemical compositions of the specimens

Sample	Composition
A1	$(Ba_{0.732}Sr_{0.26}Dy_{0.008})TiO_{3.004}$
A2	$(Ba_{0.732}Sr_{0.26}Dy_{0.008})TiO_{3.004}$+0.4 wt. % Sb_2O_3
A3	$(Ba_{0.732}Sr_{0.26}Dy_{0.008})TiO_{3.004}$+0.8 wt. % Sb_2O_3
A4	$(Ba_{0.732}Sr_{0.26}Dy_{0.008})TiO_{3.004}$+1.2 wt. % Sb_2O_3
A5	$(Ba_{0.732}Sr_{0.26}Dy_{0.008})TiO_{3.004}$+1.6 wt. % Sb_2O_3
A6	$(Ba_{0.732}Sr_{0.26}Dy_{0.008})TiO_{3.004}$+2.0 wt. % Sb_2O_3
B1	$(Ba_{0.612}Sr_{0.38}Dy_{0.008})TiO_{3.004}$+1.6 wt. % Sb_2O_3
B2	$(Ba_{0.672}Sr_{0.32}Dy_{0.008})TiO_{3.004}$+1.6 wt. % Sb_2O_3
B3	$(Ba_{0.872}Sr_{0.12}Dy_{0.008})TiO_{3.004}$+1.6 wt. % Sb_2O_3
B4	$(Ba_{0.952}Sr_{0.04}Dy_{0.008})TiO_{3.004}$+1.6 wt. % Sb_2O_3
B5	$(Ba_{0.972}Sr_{0.02}Dy_{0.008})TiO_{3.004}$+1.6 wt. % Sb_2O_3

The phases of the specimens were confirmed by X-ray diffraction (Rigaku D/max 2500 V/pc) with CuK_α radiation. The surface morphologies of the specimens were studied using a scanning electron microscope (PhilipXL30 ESEM). The electric permittivities of ceramic bodies were measured with a YY 2811 Automatic LCR Meter 4425 at 1kHz in an environment chamber with controlled temperature from –25 °C to 90 °C. And the ac standing voltages were measured with a high voltage device (CJ-2677A) at 50 Hz after the pellets had been coated with 1 mm diameter point electrodes to prevent the surface discharges.

3. Results

Figures 1–3 show the XRD patterns of $(Ba_{0.732}Sr_{0.26}Dy_{0.008})TiO_{3.004}$ ceramics with various Sb_2O_3 contents. As indicated in Fig. 1, all these samples are multiphase compounds with $Ba_{1-x}Sr_xTiO_3$ as the major phase. XRD profiles focusing on the (103)/(310) and (113)/(311) diffraction peaks are presented in Fig. 2. The (103) and (310) peaks are separated from each other for sample A1 and A2, whereas the two peaks are merged together for samples A4 and A6. The XRD peak corresponding to (113) and (311) plane exhibits a split only for sample A1. It is revealed that at room temperature the structure of major phase changes from tetragonal to cubic as the Sb_2O_3 content increases. The patterns in the 2θ range from 20° to 30° are recorded in Fig. 3. It was found that in addition to the perovskite phase, the orthorhombic compound $Ba_4Ti_{13}O_{30}$

(space group *Cmca*(64)) is precipitated as a secondary phase in samples A1 and A2. As the Sb_2O_3 content increases, the monoclinic compound $Ba_6Ti_{17}O_{40}$ (space group *C*2/*c*(15)) and the triclinic compound Ti_7O_{13} (space group $\bar{I}1(2)$) are formed consecutively in samples A4 and A6. There is no phase containing Sb, even in samples A6, implying that the dopants have entered the perovskite structure but have not contributed to the formation of secondary phases.

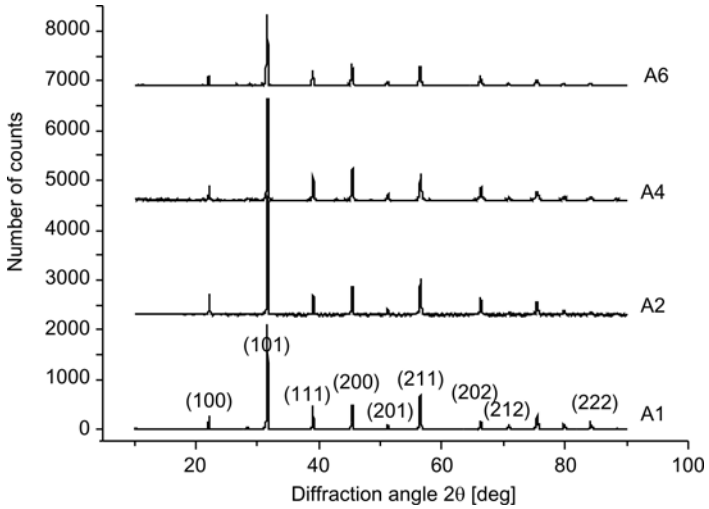

Fig. 1. XRD patterns of $(Ba_{0.732}Sr_{0.26}Dy_{0.008})TiO_{3.004}$ ceramics with various Sb_2O_3 contents; 2θ in the range 10–90°

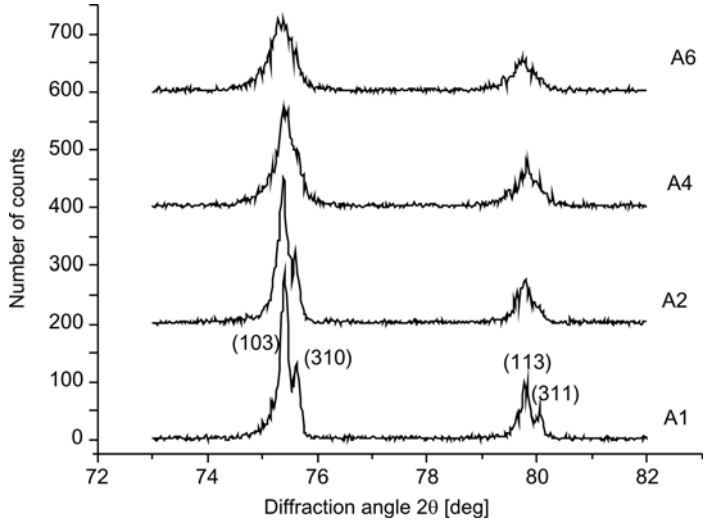

Fig. 2. XRD patterns of $(Ba_{0.732}Sr_{0.26}Dy_{0.008})TiO_{3.004}$ ceramics with various Sb_2O_3 contents; 2θ in the range 73–82°

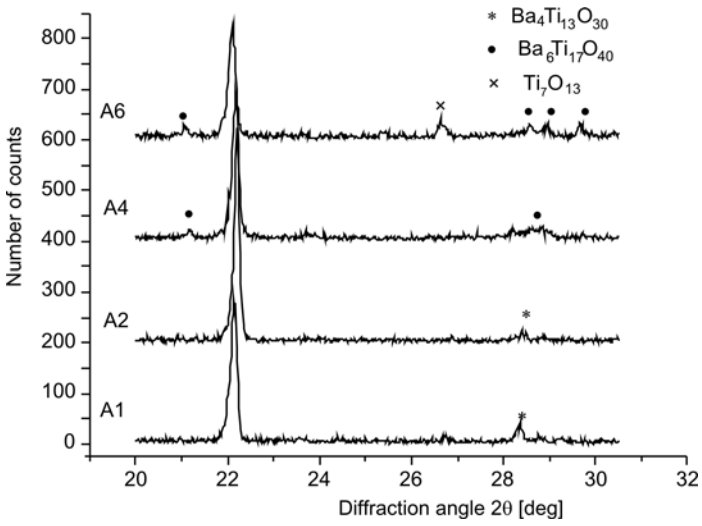

Fig. 3. XRD patterns of $(Ba_{0.732}Sr_{0.26}Dy_{0.008})TiO_{3.004}$ ceramics with various Sb_2O_3 contents; 2θ in the range 20–30.5°

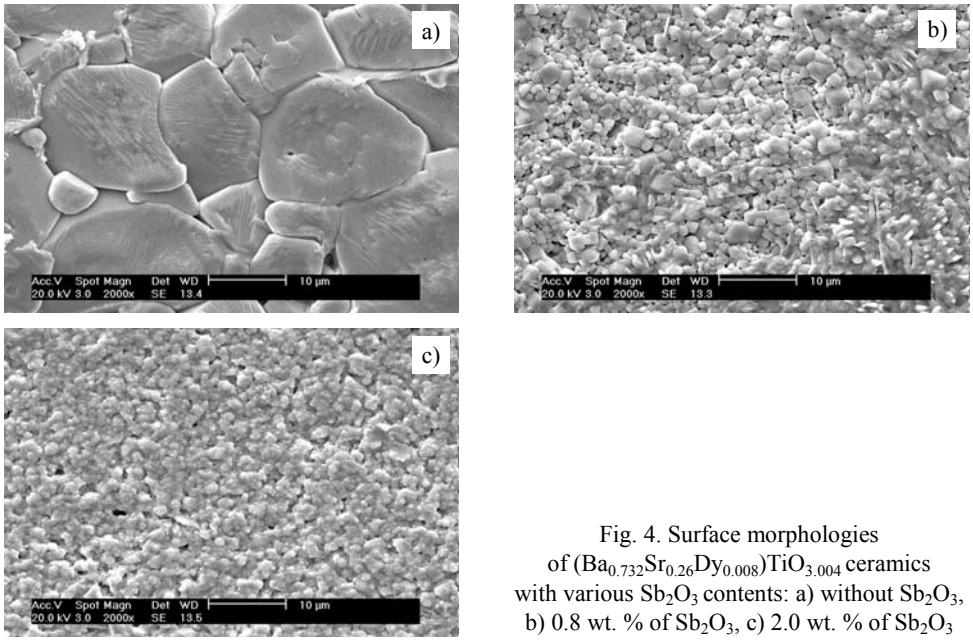

Fig. 4. Surface morphologies of $(Ba_{0.732}Sr_{0.26}Dy_{0.008})TiO_{3.004}$ ceramics with various Sb_2O_3 contents: a) without Sb_2O_3, b) 0.8 wt. % of Sb_2O_3, c) 2.0 wt. % of Sb_2O_3

The surface morphologies of $(Ba_{0.732}Sr_{0.26}Dy_{0.008})TiO_{3.004}$ ceramics with various Sb_2O_3 contents are shown in Fig. 4. It appears that all the samples exhibit a dense and uniform microstructure. The average grain size is decreased as the content of Sb_2O_3 is increased.

The structural and dielectric parameters of sintered specimens with different Sb_2O_3 contents at room temperature are shown in Table 2. It is obvious that the average lattice constant $(a^2c)^{1/3}$ where a and c are lattice parameters of the tetragonal cell decreases initially and then increases as the Sb_2O_3 content increases. The electric permittivity increases, reaches a maximum and then decreases as the Sb_2O_3 doping content increases. The dielectric loss increases at the beginning and then decreases dramatically with the increase of Sb_2O_3 content before it gets saturated. The Curie temperature decreases as the added Sb_2O_3 content increases.

Table 2. Structural and dielectric parameters of sintered specimens with various Sb_2O_3 contents

Sample	a [nm]	c [nm]	$(a^2c)^{1/3}$ [nm]	ε	tanδ	T_c [°C]
A1	0.39485	0.40115	0.39694	3295	0.009	45
A2	0.39534	0.40006	0.39691	9055	0.024	30
A3	–	–	–	6733	0.007	5
A4	0.39304	0.40140	0.39581	2498	0.007	–24
A5	–	–	–	2252	0.007	<–25
A6	0.39463	0.40156	0.39693	2054	0.007	<–25

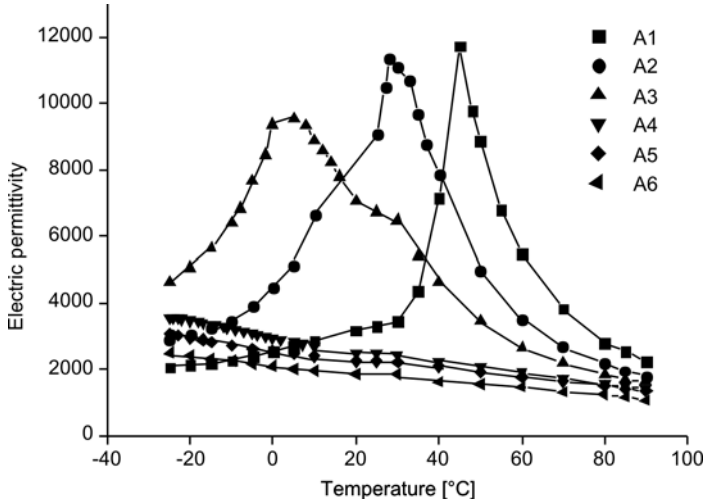

Fig. 5. Temperature dependences of electric permittivities of A1–A6 samples at 1 kHz

Figure 5 shows the temperature dependence of the electric permittivity of $(Ba_{0.732}Sr_{0.26}Dy_{0.008})TiO_{3.004}$ ceramics with various Sb_2O_3 contents. It is obvious that the permittivity of the samples is significantly suppressed as the Sb_2O_3 content increases, which is consistent with our previous findings with respect to Sb_2O_3 doped $(Ba_{0.732}Sr_{0.26}Y_{0.008})TiO_{3.004}$ system. In particular, the peak value decreases rapidly from 11 730 to 3550 for samples A1 and A4, respectively. Furthermore, at low Sb_2O_3 dop-

ing concentration (<0.8 wt. %) the curves are characterized by narrow peaks which imply high values of the temperature coefficient of capacitor (TCC). When the level of Sb_2O_3 addition reaches 2.0 wt. %, the curve becomes flat and a low TCC over a wide temperature range from –25 °C to 85 °C can be obtained.

Table 3. Dielectric parameters of sintered specimens with various Sr to Ba ratios

Sample	ε	tanδ	ρ [MΩ·mm]	E_b [kV/mm]	Tc [°C]
B1	1415	0.002	3941	5.3	<–25
B2	1600	0.003	3597	5.1	<–25
B3	2501	0.006	1130	4.4	–15
B4	3237	0.009	608	4.2	5
B5	3248	0.009	607	4.2	8

The dielectric parameters of sintered specimens with various Sr/Ba ratios at room temperature are shown in Table 3. It is evident that the Curie temperature increases with the decrease in the Sr/Ba ratio, which is consistent with many other reports [1, 16]. The resistivity and ac standing voltage decrease as the Sr/Ba ratio decreases and due to the shift of the Curie temperature towards room temperature, the electric permittivity as well as the dielectric loss increase as the Sr/Ba ratio decreases.

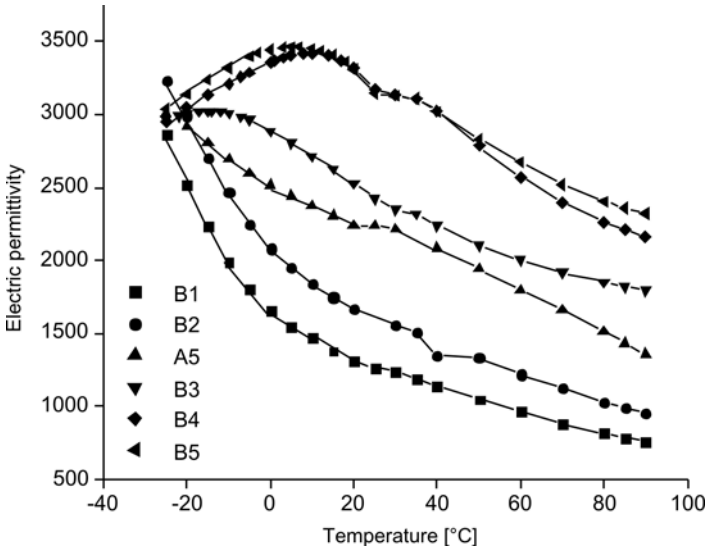

Fig. 6. Temperature dependences of electric permittivities for B1–B5 and A5 sample

Figure 6 shows the temperature dependences of the electric permittivity of ceramics with various Sr/Ba ratios. It can be seen that the curves for samples B4 and B5 are much broader than those for samples B1 and B2. This indicates that the thermal stabil-

ity of the electric permittivity for samples increases with the decrease in the Sr/Ba ratio.

4. Discussion

As shown in Table 2, the average lattice constant $(a^2c)^{1/3}$ decreases initially and then increases as the Sb_2O_3 content increases. This demonstrates that Sb^{3+} ions (0.076 nm) first substitute the bigger Ba^{2+} ions (0.161 nm) or Sr^{2+} ions (0.144 nm) and then replace the smaller Ti^{4+} ions (0.061 nm). Thus the substitution characteristic of Sb_2O_3 in $(Ba_{0.732}Sr_{0.26}Dy_{0.008})TiO_{3.004}$ ceramics is similar to that of Sb_2O_3 in Y-doped BST dielectrics [15]. When Sb^{3+} ions occupy the A sites and serve as donor dopants, the defect reaction is as follows:

$$Sb_2O_3 \rightarrow 2Sb_A^{\bullet} + V_A^{''} + 3O_O \tag{5}$$

With the increase of Sb_2O_3 concentration, Sb^{3+} ions begin to enter B sites and serve as acceptor dopants. The defect reaction can be expressed as follows:

$$Sb_2O_3 \rightarrow 2Sb_B^{\prime} + V_O^{\bullet\bullet} + 3O_O \tag{6}$$

The above models are similar to those proposed by Sasaki et al. [17] for $BaTiO_3$ thin films with high Sb doping concentration:

$$Sb_2O_3 + 3TiO_2 \rightarrow 2Sb_{Ba}^{\bullet} + 3Ti_{Ti} + 9O_O + V_{Ba}^{''} \tag{7}$$

and/or

$$Sb_2O_3 + 2BaO \rightarrow 2Sb_{Ti}^{\prime} + 2Ba_{Ba} + 5O_O + V_O^{\bullet\bullet} \tag{8}$$

The substitution for A site or B site with any of the Sb^{3+} ions leads to a shorter distance between the central ion and its nearest neighbours of the octahedron, thus the movement of the central ion is confined which weakens the spontaneous polarization of the grain lattice, and consequently, the Curie temperature decreases as the Sb_2O_3 content increases. The charged vacancies caused by A site and B site substitution give rise to the local deformation of the perovskite unit cells which also causes the reduction of the Curie temperature. It is well known that the electric permittivity and dielectric loss near the phase transition region usually exhibit high values. Therefore, the shift of the Curie temperature is expected to be the main reason for variation of the electric permittivity and dielectric loss.

The influence of Sb_2O_3 addition on the temperature dependence of the permittivity is caused by the weakening of ferroelectricity which is attributed to the replacement reaction of Sb^{3+} ions for the host cations in the perovskite lattice.

As shown in Fig. 6, the lower Sr/Ba ratio is, the flatter the temperature variation curve becomes. The broadening of the curve is attributed to the disorder in the arrangement of cations at the A site which leads to a microscopic heterogeneity in the composition, and thus results in a continuous phase transition of different tiny regions. A considerable decrease in the ac standing voltage shown in Table 3 is ascribed to the increasing proportion of tiny regions which undergo the transitions between tetragonal and cubic phases at room temperature. In other words, it is basically because of the shift of the Curie temperature towards the room temperature as the Sr/ Ba ratio decreases. Due to its high permittivity (ε = 3248), acceptable dielectric loss (tanδ = 0.009*)*, high ac standing voltage (E_b = 4.2 kV/mm) and low TCC (< ±25%), the sample B5 is promising for applications in environment friendly capacitors.

5. Conclusions

Dielectric ceramics based on Sb_2O_3 doped $(Ba_{0.992-x}Sr_xDy_{0.008})TiO_{3.004}$ were prepared through a conventional solid state reaction technique and their dielectric properties were investigated. The doping content of Sb_2O_3 and the Sr/Ba ratio were both varied. XRD patterns confirmed these ceramics to be multiphase compounds with perovskite major phase. The average lattice constant indicates that Sb^{3+} ions first substitute the A site ions and then replace the B site ions. The Curie temperature decreases as the Sb_2O_3 content and Sr/Ba ratio increase. The temperature dependence of the electric permittivity increases as the Sb_2O_3 concentration increases but decreases with the increase in the Sr/Ba ratio. Sintered samples with high Sb_2O_3 doping level and low Sr/Ba ratio in the Sb_2O_3 doped $(Ba_{0.992-x}Sr_xDy_{0.008})TiO_{3.004}$ system exhibit more satisfactory dielectric properties compared with previous ceramics .

Acknowledgement

This work was supported by the Chinese Doctor Foundation of National Ministry of Education (Grant No. 20040056055).

References

[1] FU C.L., YANG C.R., CHEN H.W., WANG Y.X., HU L.Y., Mater. Sci. Eng. B, 119 (2005), 185.
[2] JEON J.H., HAHN Y.D., KIM H.D., J. Eur. Ceram. Soc., 21 (2001), 1653.
[3] WEI X.Y., YAO X., Mater. Sci. Eng. B, 99 (2003), 74.
[4] ABDELKEFI H., KHEMAKHEM H., VÉLU G., CARRU J.C., MÜHLL R.V., J. Alloys Compd., 399 (2005), 1.
[5] ALEXANDRU H.V., BERBECARU C., IOACHIM A., NEDELCU L., DUTU A., Appl. Surf. Sci., 253 (2006), 354.
[6] IOACHIM A., TOACSAN M. I., BANCIUM.G., NEDELCU L., DUTU A., ANTOHE S., BERBECARU C., GEORGESCU L., STOICA G., ALEXANDRU H.V., Thin Solid Films, 515 (2007), 6289.
[7] LI R.X., CHENG J.R., MENG Z.Y., WU W.B., J. Mater. Sci.-Mater. Electron., 17 (2006), 587.
[8] LIU S.J., ZENOU V.Y., SUS I., KOTANI T., SCHILFGAARDE M., NEWMAN N., Acta Mater., 55 (2007), 2647.

[9] HUANG X.Y., GAO C.H., CHEN X.C., ZHENG X.L., HUANG G.J., LIU H.P., J. Rare Earths, 22 (2004), 226.
[10] ZHAO C., HUANG X.Y., GUAN H., GAO C.H., J. Rare Earths, 25 (2007), 197.
[11] KIM J.H., YOON S.H., HAN Y.H., J. Eur.Ceram. Soc., 27 (2007), 1113.
[12] LI Z.C., ZANG H., ZOU X., BERGMAN B., Mater. Sci. Eng. B, 116 (2005), 34.
[13] MIAO H.Y., DONG M., TAN G.Q., PU Y.P., J. Electroceram., 16 (2006), 297.
[14] KIM I.H., LEE H.W., KIM Y.M., KIM H.J., UR S.C., Mater. Lett., 60 (2006), 3027.
[15] ZHANG C., QU Y.F., MA S.C., Mater. Sci. Eng. B, 136 (2007),118.
[16] PATIL D.R., LOKARE S.A., DEVAN R.S., CHOUGULE S.S., KANAMADI C.M., KOLEKAR Y.D., CHOUGULE B.K., Mater. Chem. Phys., 104 (2007), 254.
[17] SASAKI Y., FUJII I., MATSUI T., MORII K., Mater. Lett., 26 (1996), 265.

Received 15 June 2008
Revised 31 March 2009